

Visual Detection of Diver Attentiveness for Underwater Human-Robot Interaction*

Sadman Sakib Enan¹ and Junaed Sattar²

ABSTRACT

Many underwater tasks, such as cable-and-wreckage inspection, search-and-rescue, benefit from robust human-robot interaction (HRI) capabilities. With the recent advancements in vision-based underwater HRI methods, autonomous underwater vehicles (AUVs) can communicate with their human partners even during a mission. However, these interactions usually require active participation especially from humans (*e.g.*, one must keep looking at the robot during an interaction). Therefore, an AUV must know when to start interacting with a human partner, *i.e.*, if the human is paying attention to the AUV or not. In this paper, we present a diver attention estimation framework for AUVs to autonomously detect the *attentiveness* of a diver and then navigate and reorient itself, if required, with respect to the diver to initiate an interaction. The core element of the framework is a deep neural network (called DATT-Net) which exploits the geometric relation among 10 facial keypoints of the divers to determine their head orientation. Our on-the-bench experimental evaluations (using unseen data) demonstrate that the proposed DATT-Net architecture can determine the attentiveness of human divers with promising accuracy. Our real-world experiments also confirm the efficacy of DATT-Net which enables real-time inference and allows the AUV to position itself for an AUV-diver interaction.

1 INTRODUCTION

In recent years, AUVs have been used in independent missions (*e.g.*, underwater oil spill survey system [32], oceanographic survey system [20]), and also increasingly in collaborative settings containing both humans and other AUVs (*e.g.*, [22, 34]). The ever-increasing on-board computing power, availability of low-cost and affordable AUVs, and improved HRI capabilities are some of the contributing factors behind the surge in AUV usage. Currently, humans and AUVs can effectively interact with each other using a number of different methods, such as high-speed tethered communication [4], fiducial markers [31], gesture-based framework [21], small displays and lighting schemes [6], and motion-based methods [13]. But these interaction systems usually require both the diver and the AUV to be oriented properly and to be in close proximity to each other. And, almost all of the time it is the diver who swims towards the AUV, orients themselves correctly with respect to the AUV, and begins the interaction. However, this puts additional physical and cognitive burdens on the divers. On the other hand, AUVs do not currently have this capability as it is extremely difficult for a machine to intelligently perceive human orientation and attention underwater, localize itself and the target, navigate towards the target, and reorient itself all at the same time. This is mainly due to

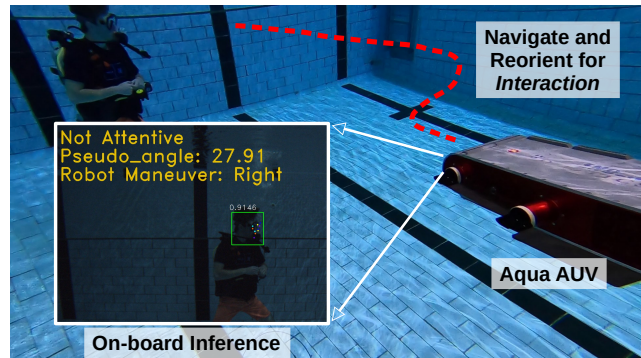


Figure 1: Demonstration of the proposed diver attention estimation framework where the AUV detects an inattentive diver in real-time. The dashed red line demonstrates the trajectory the robot intends to take to position itself with respect to the diver to initiate interaction. The detection probability and the predicted keypoints (on the inset) are best viewed at 200% zoom or above.

the domain-specific challenges underwater, *e.g.*, degraded visuals, reduced sensing capability arising from signal attenuation, less reliable localization and motion planning, and lack of high-bandwidth wireless communication. Nevertheless, AUVs are successfully using their visual perception capabilities in littoral regions owing to the success of underwater vision improvements [11] and novel deep learning innovations [23]. This success contributes to the development of the work in [14], which proposes to use monocular cameras to approach a human diver by leveraging the pose of the body and biological priors to facilitate human-robot interaction. This method does not require the use of expensive sensors, such as stereo cameras, sonar, acoustic sensors (*e.g.*, Doppler Velocity Logs), and localization devices, and yet achieves promising results. However, the proposed solution always assumes that a diver is ready to interact. There are times when a diver may be engaged in a different task or interaction with a fellow dive buddy but is still willing to interact with a robot only if the robot positions itself conveniently. In such scenarios, it is imperative for the AUVs to understand the intent of the diver, more specifically their attentiveness. *In the context of the paper, we use the phrases ‘diver attention’ and ‘attentiveness of the diver’ interchangeably, which refer to whether or not a diver is looking at a robot with an intention to interact and/or collaborate.*

In this work, we present a novel diver attention estimation framework which will enable an AUV to detect the attentiveness of a diver. If the diver is attentive, the AUV signals its intention to begin interaction immediately. If the diver is not attentive, the AUV navigates and reorients itself as necessary to show its intention to interact with the diver. To determine the attentiveness of the diver, however, the AUV needs to know the head orientation or

The authors are with the Department of Computer Science & Engineering and the Minnesota Robotics Institute, University of Minnesota, MN, USA. {¹enan0001, ²junaed}@umn.edu.

*This work was supported by a University of Minnesota UMII-MnDRIVE Fellowship.

the head pose of the diver. In terrestrial applications, researchers solve 3D (head) pose estimation problems using various learning algorithms (e.g., [25, 26, 29]), which use datasets that contain 3D locations of the pose keypoints with respect to a global frame. However, there are no datasets that contain 3D head pose data of scuba divers, partly arising from the difficulty and logistical challenges in collecting such datasets. In contrast, some researchers model the 3D pose estimation problem as a 2D problem, and have used keypoints regression to address the 3D pose estimation challenge [3, 5]. However, it is almost impossible to estimate the 3D pose from a 2D image if the corresponding 2D keypoints are not even visible in the image space. Consequently, the unseen keypoints are not even annotated in the datasets and are not used in establishing the 2D-3D correspondence. In our work, we propose to tackle this unique problem by creating the very first Diver Attention (DATT) dataset which contains a wide collection of annotated diver images. We carefully annotate the diver face bounding box and 10 facial keypoints in a way that the keypoints represent the orientation of the head in the image space. In fact, we annotate the facial keypoints even if the frontal face is not fully visible to promote learning of the geometric structure of the keypoints, as opposed to only the individual keypoints location. In addition, we design a deep neural network architecture (DATT-Net) which can be supervised to learn the spatial location of the 10 facial keypoints. Finally, we use the detected keypoints to estimate the attentiveness of a scuba diver and design a robot controller for the Aqua AUV [9] to navigate and reorient itself with respect to a diver to begin an interaction (as shown in Fig. 1).

We make the following contributions in this paper:

- (1) We present the DATT dataset containing 3,314 annotated diver images, collected during multiple closed-water robot trials. The images are carefully annotated to include diver face bounding boxes and 10 facial keypoints of divers.
- (2) We propose an end-to-end deep neural network called DATT-Net to capture diver faces and their associated facial keypoints even if a diver is looking at a 90 degree angle with respect to the camera. The training pipeline includes a multi-loss objective function which gives emphasis on maintaining the actual geometric relation among the facial keypoints.
- (3) We perform spread analysis on the facial keypoints to determine the attentiveness of a diver and define a *pseudo*-angle variable to quantify the direction of diver’s attention.
- (4) We perform a number of qualitative and quantitative experiments that validate that the proposed framework can robustly estimate the attentiveness of the diver.
- (5) We deploy the proposed algorithm on a physical AUV and further design a controller which helps navigate and reorient the AUV to position itself for interaction with a human diver when required.

2 DATT DATASET

To facilitate the training and testing of the proposed diver attention estimation system, we prepare a diver attention (DATT) dataset which contains a wide variety of annotated underwater diver images. The images have a resolution of 1920×1080 pixels and are collected from multiple closed-water pool trials using GoPro action

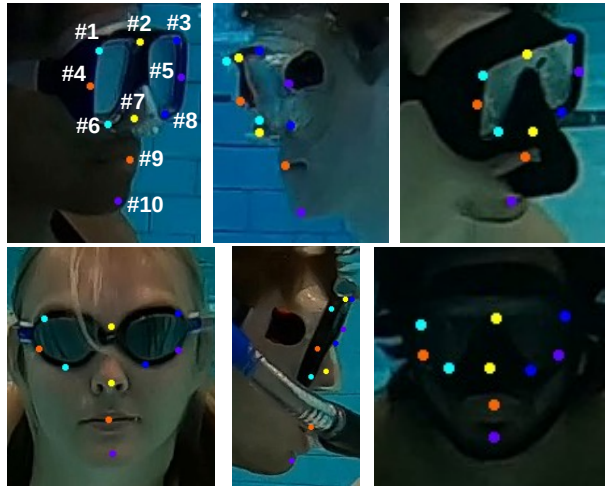


Figure 2: Six annotated samples from the DATT dataset where the divers are wearing different types of scuba gear and are looking at different directions. Each annotation includes four bounding box coordinates and 10 facial keypoints coordinates. Here, the demonstrated samples are cropped using their bounding box values.

cameras [1]. There are a total of 3,314 annotated diver images. To increase the diversity of the dataset, the divers were instructed to appear differently underwater. Some divers wore scuba masks while others simply put on pairs of goggles. Some used their snorkels while a few others did not. The head orientation of the divers were also varied by instructing them to look directly at the camera or to look elsewhere at different angles (both in the left and right directions). As a result, there are even instances where the faces of the divers are completely obscured from the camera’s perspective, i.e., the diver is looking to their left or right at a 90 degree angle with respect to the camera.

Since we want to identify the head orientation of the divers directly from the 2D images, we carefully annotate the images to reflect as much 3D perspective properties as possible. We start by annotating the diver face bounding boxes. To determine the head orientation of the diver, a full set of facial keypoints and their underlying geometrical relationships need to be used. Traditionally, researchers select eyes and two corners of the lips, among others, as three of the vital facial keypoints for terrestrial applications. However, for a diver underwater, their eyes are usually obscured by the scuba mask or goggles and the shape of their lips are mostly distorted by the snorkels or regulators. So, instead of selecting facial keypoints in the traditional manner, we leverage the following facts. Since the breathing apparatus on the face (e.g., masks and regulators) are always visible underwater and are rigid types of objects, we select most of our facial keypoints on those and focus mainly on finding the geometry of the facial keypoints to mimic the shape of those in 3D space. Specifically, we select 10 facial keypoints which are easier to identify underwater compared to the traditional facial keypoints where eight keypoints are on the mask, one is on the snorkel or regulator, and the remaining keypoint is

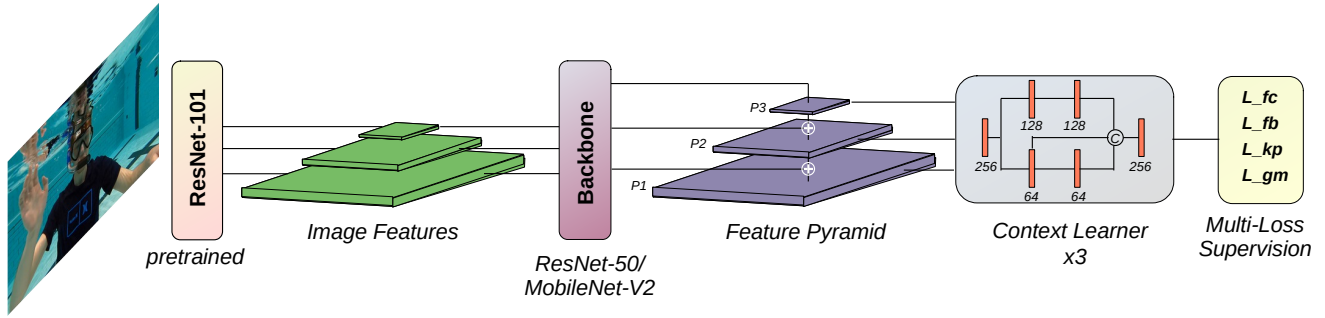


Figure 3: Network architecture of the proposed model. DATT-Net employs a multi-scale learning on a feature pyramid and has an extra supervision branch to learn the geometric relation of facial keypoints. This allows the algorithm to work even if the diver is distant and facing at a 90 degree angle with respect to the robot.

on the diver’s chin. We always annotate all 10 facial keypoints even if some of them are not visible so that a downstream algorithm can regress the keypoints based on the actual geometric relation among the keypoints. Fig. 2 shows a few annotated samples from the DATT dataset.

3 DATT-NET

The goal of the proposed diver attention estimation framework is to calculate the head orientation of a scuba diver to determine if they are attentive to a companion robot. To achieve this, we have to- (1) localize diver faces, (2) determine the facial keypoints of the diver, and (3) estimate the head orientation (*i.e.*, attentiveness) from the geometry of the keypoints. In this paper, we propose to solve the first two of these tasks with a unified architecture, called DATT-Net, in a supervised manner. Inspired by the robust single-stage face detector named RetinaFace [8], we design DATT-Net as follows.

3.1 Feature Extractor

DATT-Net uses a ResNet-101 block [18], pretrained on ImageNet dataset [7], to extract the initial features from the input image of 640×640 resolution. Since we want to identify the diver faces and consequently the facial keypoints of the divers regardless of their physical distance from the robot, we employ a multi-scale learning approach as was used in [17]. Therefore, we extract the initial features at three different scales (*i.e.*, from three different layers of ResNet-101). These features are further refined individually using a backbone network (we use either ResNet-50 [18] or MobileNet-V2 [30] as the backbone). We refrain from using any pretrained weights for the backbone network to eliminate any learning biases from the ImageNet dataset. We then create a three-level (P_1, P_2, P_3) feature pyramid [24] with these extracted features using both top-down and lateral connections, as described in [8]. Instead of performing the final predictions directly on the feature pyramid, we use extra context learning modules to leverage information from the surrounding pixels. It is shown in [27] that using such post-context learning blocks increases the receptive fields of the pixel locations, which enables knowledge from the surroundings and hence gives better inference. The outputs from the final

three context modules have feature dimensions of $(80 \times 80 \times 256)$, $(40 \times 40 \times 256)$, and $(20 \times 20 \times 256)$, respectively.

3.2 Facial Anchors

To capture the facial keypoints of the divers at different scales, we perform the network supervision at patch levels on the feature pyramid. These patches, called *anchors*, were introduced in [33] for enabling multi-scale face detection. Since underwater human-robot interaction takes place at a reasonably close distance, we select 16 as the smallest anchor size to capture distant divers. As for the rest, we use anchors of sizes 32, 64, 128, and 256. Anchors 16 and 32 work on level P_1 , 64 and 128 on level P_2 , and finally the anchor 256 works on level P_3 . All the anchors have square dimensions. We consider an anchor to have a diver face if it matches with the ground truth bounding box with an Intersection over Union (IoU) value of at least 60% and to have background if the IoU is less than 0.4. All other anchors are ignored.

3.3 Objective Function Formulation

One of the primary goals of this work is to accurately identify the facial keypoints even if they are invisible in the image space. Therefore, we formulate the objective function as a multi-loss optimization problem (as was used in [16]) where we not only want to detect diver faces and their facial keypoints but also maintain the underlying geometric relation among the 10 keypoints. The individual loss components are described below:

- (1) $\mathcal{L}_{fc}(f, f_{gt})$: This is a *cross-entropy loss* which governs whether a particular image patch (anchor) is a face or background. Here, f is the probability of an anchor being a face. If, for an anchor, the ground truth also contains a face, then the value of f_{gt} is 1 otherwise it is 0. Here, gt refers to the ground truth values.
- (2) $\mathcal{L}_{fb}(\vec{b}, \vec{b}_{gt})$: This is the *diver face bounding box regression loss* where $\vec{b} = [x_{min}, y_{min}, x_{max}, y_{max}]$ is a vector containing the predicted face bounding box coordinates. Here, \mathcal{L}_{fb} is a smooth- L_1 loss which was introduced in [16] and is defined as,

$$\text{smooth-}L_1(x) = \begin{cases} 0.5x^2 & \text{if } |x| \leq 1 \\ |x| - 0.5 & \text{otherwise} \end{cases} \quad (1)$$

where x is fed as the difference between the predicted and the ground truth bounding box coordinates. Finally, the loss is averaged for all four coordinates.

- (3) $\mathcal{L}_{kp}(\vec{p}, \vec{p}_{gt})$: This is the *diver face keypoints regression loss* where $\vec{p} = [x_1, y_1, \dots, x_{10}, y_{10}]$. The loss is also calculated as a smooth- L_1 loss (as shown in Eq. 1). Essentially, \mathcal{L}_{kp} supervises the algorithm to predict the 10 facial keypoints closer to the ground truth values. For both \mathcal{L}_{fb} and \mathcal{L}_{kp} losses, the four bounding box coordinates and the 10 facial keypoints values were normalized.
- (4) $\mathcal{L}_{gm}(\vec{p})$: Finally, we introduce an additional *geometric loss* term which enforces the algorithm to maintain the geometric relation among the 10 keypoints. This should allow accurate keypoints regression even if all 10 keypoints are not visible in the image space. This is a vital criteria because we want our algorithm to infer accurate facial keypoints even if the diver is looking at a 90 degree angle with respect to the robot’s camera. Since scuba masks are rigid types of object, the points on a mask should never deviate from their relative positions (with respect to one another) in a 3D space regardless of the head orientation of the diver. We leverage this idea on image space and ensure that the outer six keypoints ($p_1, p_3, p_4, p_5, p_6, p_8$) on the scuba masks are symmetric with respect to the middle two keypoints (p_2, p_7). We define the loss term as,

$$\mathcal{L}_{gm}(\vec{p}) = \sum_{j=2,7} l(p_{1j}, p_{3j}) + l(p_{4j}, p_{5j}) + l(p_{6j}, p_{8j})$$

where

$$l(p_{ab}, p_{cb}) = |d_{p_{ab}} - d_{p_{cb}}|$$

$$\text{and, } d_{p_{mn}} = \sqrt{(x_m - x_n)^2 + (y_m - y_n)^2}$$

In total, we minimize the following multi-loss objective function:

$$\mathcal{L} = \mathcal{L}_{fc} + \alpha f_{gt} \mathcal{L}_{fb} + \beta f_{gt} \mathcal{L}_{kp} + \gamma f_{gt} \mathcal{L}_{gm} \quad (2)$$

where α, β, γ are set to 0.2, 0.15, and 0.1, respectively. As can be seen from Eq. 2, the last three loss terms are only taken into account if an anchor contains a face (*i.e.*, $f_{gt} = 1$). Fig. 3 shows the complete architecture of DATT-Net.

3.4 Implementation Details

We use TensorFlow [2] libraries to implement DATT-Net. All the input images are resized to have 640×640 resolution. To augment the DATT dataset, we utilize the following schemes (as suggested in [19, 35]): random cropping, image flipping, normalization, image distortion (varying the brightness, hue, saturation, contrast, and sharpness), etc. During training, we use a batch size of 8, learning rate of 10^{-2} with a scheduler which lowers the value down to 10^{-5} , and stochastic gradient descent (SGD) as the optimizer with a momentum of 0.9. We have trained the network using 2, 652 training images on an Nvidia GeForce RTX 2080 GPU for 300 epochs where we noticed convergence in the validation loss. For testing, we have used an Intel® Xeon® E5-2650 CPU for bench operation and an Intel® i3-6100U CPU (of the Aqua AUV) for on-board deployment.

4 DIVER ATTENTION ESTIMATION

We estimate the attentiveness of a scuba diver using DATT-Net’s prediction of the 10 facial keypoints. First, we measure the x -spread of the outer keypoints on the scuba mask ($p_1, p_3, p_4, p_5, p_6, p_8$) with respect to the nose (p_7) of the diver. However, instead of directly comparing against the nose coordinate, we use the mean (x_{mean}) location of the inner keypoints (p_2, p_7, p_9, p_{10}) because these points should always lie on the same line in a 3D space. We use,

$$x\text{-spread} = \frac{1}{6} \sum_{i=1,3,4,5,6,8} \sqrt{(x_{p_i} - x_{mean})^2}$$

to compute the spread. We normalize the x -spread value with respect to the width of the predicted diver face bounding box. Second, we leverage the positions of the top three keypoints (p_1, p_2, p_3) on the diver’s mask with respect to center (x_{center}) of the face bounding box to define a *pseudo-angle* variable to quantify the angular deviation of a diver’s head from the center; *pseudo-angle* is defined as

$$pseudo\text{-angle} = x_{mask} - x_{center}$$

where x_{mask} is the mean x location of the keypoints p_1, p_2, p_3 .

Finally, we determine the attentiveness (*att*) of a diver as follows,

$$att = \begin{cases} True & \text{if } x\text{-spread} > \lambda_1 \text{ and } |pseudo\text{-angle}| < \lambda_2 \\ False & \text{otherwise} \end{cases}$$

where the values of λ_1 and λ_2 are empirically found as 0.27 and 10, respectively. Also, we conclude that a diver is looking to their left if *pseudo-angle* > 0 and right if *pseudo-angle* < 0 .

5 ROBOT CONTROLLER

To design a controller for an AUV to use the *pseudo-angle* to navigate and reorient itself for interaction with a diver, we choose the six-legged Aqua robot platform. We create a Robot Operating System (ROS) [28] package consisting of two nodes; one of these continuously predicts the facial keypoints to estimate the diver attention, and the other node keeps track of the attentiveness of the diver for the past 3 seconds. Based on the recent attentiveness (*Attentive*, *Looking Right*, or *Looking left*) score, we design our algorithm to make the Aqua AUV autonomously navigate and reorient itself to interact with the diver if required (*i.e.*, if the diver is looking right, the AUV must do a left maneuver, and vice-versa). We implement the maneuvers using a motion controller introduced in [15]. The initial turn, circular movement, and the final turn are governed by the *pseudo-angle* value.

6 EXPERIMENTAL EVALUATIONS

To evaluate the performance of the diver attention estimation framework, we run DATT-Net on the test set of DATT dataset which contains 662 diver images. We also run DATT-Net on 150 images extracted from data collected through multiple closed-water robot trials which were captured using a data collection device equipped with USB 3.0 stereo cameras [10] and Aqua AUV’s uEye cameras [9]. Furthermore, we deploy the proposed algorithm on-board the Aqua AUV in a real-world scenario (during a closed-water robot trial) and evaluate the efficacy of the algorithm with scuba divers present in the field of view of the robot. Finally, we test the performance of

Table 1: Comparison of average precision (AP) and mean AP (mAP) on both DATT test set and images extracted during closed-water robot trials.

Method	AP (%)	mAP (%)
RetinaFace	70.81	48.33
Ours (backbone: ResNet-50)	91.75	72.56
Same w/o $\mathcal{L}_{gm}(\vec{p})$	82.64	55.22
Ours (backbone: MobileNet-V2)	87.93	55.33
Same w/o $\mathcal{L}_{gm}(\vec{p})$	75.37	50.22

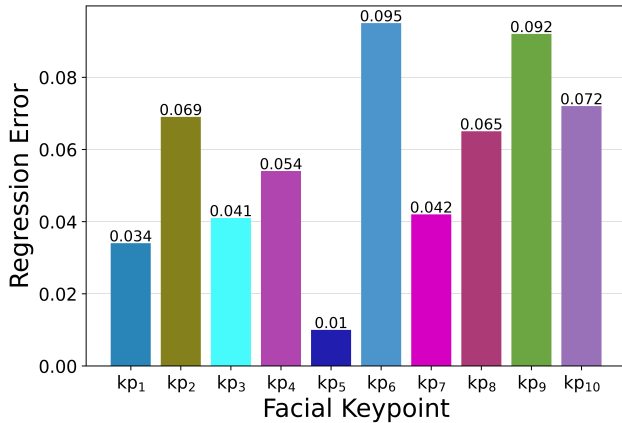


Figure 4: A bar plot showing the regression error for each of the 10 facial keypoints.

our robot controller which helps navigate and reorient the Aqua AUV for interacting with a diver, if required.

6.1 Results

6.1.1 Diver Face Detection and Keypoints Regression. Since a major component of the proposed algorithm is diver face detection, we start by comparing the diver face detection performance of DATT-Net against the state-of-the-art (SOTA) face detection algorithm (RetinaFace [8]). Specifically, we compute the average precision (AP) for IoU=0.5 and mean average precision (mAP) for IoU=[0.5:0.05:0.95]. The results are presented in Table 1. We can see that DATT-Net, regardless of the backbone network in use, achieves significantly better performance than RetinaFace. Even though RetinaFace uses additional five facial landmarks to robustly detect faces, it did not to detect underwater diver faces well. This might be due to divers wearing different types of scuba gear, as RetinaFace performed well for divers who did not wear masks, snorkels, or regulators (e.g., wearing only a pair of goggles). Furthermore, it is also evident from the table that the use of the additional supervision in the form of geometric loss contributes to better diver face detection because the AP value decreases if geometric loss is excluded during the training of DATT-Net. DATT-Net achieves the best performance (AP=91.75%, mAP=72.56%) when ResNet-50 is used as the backbone network.

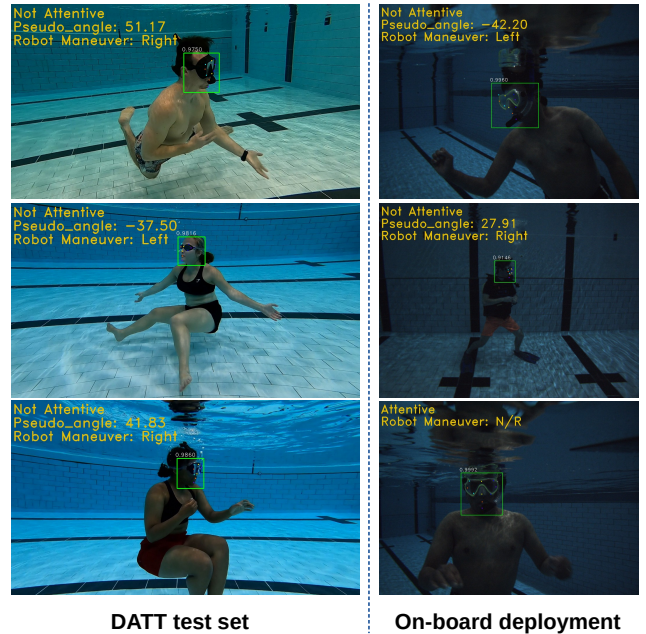


Figure 5: Qualitative performance of the proposed diver attention estimation scheme when run on (unseen) DATT test set vs. when deployed on-board actual AUV. Note the robustness of the algorithm as it works at different distances and even in poor lighting conditions (see the on-board deployment scenarios on the right column). The detection probability and the predicted keypoints are best viewed at 200% zoom or above.

To evaluate the performance of DATT-Net in predicting the 10 facial keypoints on DATT test set, we compute the regression errors by comparing the predictions with the corresponding ground truth. Fig. 4 presents a bar plot showing the regression errors for all 10 facial keypoints. From the figure, we notice that the regression errors are always less than 10%, with an average regression error of 5.7%. This infers that the keypoints regression loss and the geometric loss are enforcing DATT-Net to robustly regress the diver face keypoints.

6.1.2 Diver Attention Estimation. First, we perform qualitative evaluation on the performance of the proposed diver attention estimation technique. We test our algorithm on both the DATT test set (unseen data) and on-board Aqua AUV during a closed-water trial. Fig. 5 presents the qualitative results. From the figure we see that the proposed algorithm can accurately estimate the attentiveness of a diver irrespective of the type of scuba gear they are wearing. It is also evident that the proposed solution works at different distances and in various lighting conditions. This is understandable because we used multi-scale learning (using different sizes of anchors) on a feature pyramid and image distortion as a data augmentation scheme, respectively, during the training of DATT-Net (as described in Sec. 3.2 and Sec. 3.4). Additionally, the algorithm still works even if the majority of the diver’s face is not visible due

Table 2: Performance comparison of the diver attention estimation between the proposed method and a baseline approach.

Method	Baseline	Ours
Accuracy (%)	45.07	89.41

to them looking at a 90 degree angle with respect to the AUV. That means, DATT-Net is indeed benefiting from learning the keypoints geometry.

Second, we quantitatively evaluate the performance of the proposed method against a baseline. We prepare the baseline as follows. We sketch a 3D model of the head of a scuba diver wearing a scuba mask and a snorkel. We define 10 3D points in the face model in the same locations as the facial keypoints found in DATT dataset. Then, we use the predicted 10 facial keypoints from DATT-Net and the corresponding 3D points from the face model to estimate the head pose (translation and rotation vectors) using the Perspective-n-Point (PnP) algorithm [12]. Finally, we compute the angular deviation of keypoint #7 (nose) from its pose and estimate attentiveness of the diver. We run both the proposed algorithm and the baseline on the DATT test set and the 150 diver images collected from closed-water trials. Table 2 presents the results. We see that the proposed algorithm achieves a superior accuracy of 89.41% compared to the baseline (45.07%) in estimating the correct state of diver attentiveness.

6.1.3 Robot Controller’s Performance. Although the performance of our proposed diver attention estimation technique is quite robust, the current state of our robot controller is still a work in progress. During the attention estimation step, the Aqua AUV seemed to slightly pitch up which we think is because of the water current generated by a nearby pool jet. As a result, the AUV sometimes lost the diver from its field of view which resulted in a brief halt in the diver attention estimation algorithm. As soon as the AUV saw the diver, it was able to determine their attentiveness correctly every time and started to navigate towards the diver, reorient itself, and begin a diver-AUV interaction.

6.2 Limitations of the Proposed Framework

Our method relies on the prediction of the diver face bounding box. If the predicted bounding box does not include any faces, then all the subsequent modules fail. Although the performance of DATT-Net in detecting diver faces is very robust, we still see a few failure cases (as demonstrated in Fig. 6). As can be seen from the figure, the algorithm mistakenly found a diver face in the water reflection and also mistook a lane marking as a face on the swimming pool floor.

Also, the current robot controller is designed to only change its yaw value during the navigation-and-reorientation phase. That is, our controller makes an assumption that the diver-AUV interaction will happen at a fixed height in the water column. Furthermore, we have noticed that the Aqua AUV was slightly pitching up during the reorientation phase, which suggests that further controller tuning is required.

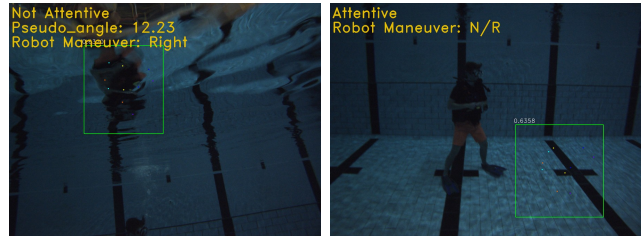


Figure 6: Two examples of diver attention estimation failures where the algorithm incorrectly detects a diver face in the reflection on the water surface (left image) and in the floor of the pool (right image). The detection probability and the predicted keypoints are best viewed at 200% zoom or above.

7 CONCLUSION

In this work, we present the design and implementation of a diver attention estimation framework to facilitate underwater diver-robot interaction. With on-the-bench experiments and closed-water trials, we show that our proposed diver attention estimation algorithm is able to determine the head orientation of the divers (*i.e.*, their attentiveness) by understanding the geometric relation among 10 facial keypoints. We also show that an AUV can leverage the attentiveness of a diver to navigate and reorient itself to initiate a diver-AUV interaction. The key advantages of our method are that it can detect the attentiveness of the divers using only a monocular camera, works at various distances and lighting conditions, does not need to know the global position of the diver to work, and is invariant to different types of scuba gear. This algorithm will serve as a step toward learning the overall intent of a scuba diver so an AUV can take more informed decision when collaborating with a diver. As an immediate next step, we will tune our robot controller so it can plan the navigation-and-reorientation task more accurately and efficiently, with full 6-degrees-of-freedom control of the robot’s motion.

REFERENCES

- [1] 2020. GoPro Hero 9. <https://gopro.com/en/us/>.
- [2] Martin Abadi, Paul Barham, Jianmin Chen, Zhifeng Chen, Andy Davis, Jeffrey Dean, Matthieu Devin, Sanjay Ghemawat, Geoffrey Irving, Michael Isard, Manjunath Kudlur, Josh Levenberg, Rajat Monga, Sherry Moore, Derek G. Murray, Benoit Steiner, Paul Tucker, Vijay Vasudevan, Pete Warden, Martin Wicke, Yuan Yu, and Xiaoqiang Zheng. 2016. TensorFlow: A System for Large-Scale Machine Learning. In *Proceedings of the 12th USENIX Conference on Operating Systems Design and Implementation (Savannah, GA, USA) (OSDI’16)*. USENIX Association, USA, 265–283.
- [3] Mykhaylo Andriluka, Stefan Roth, and Bernt Schiele. 2010. Monocular 3D pose estimation and tracking by detection. In *2010 IEEE Computer Society Conference on Computer Vision and Pattern Recognition*. 623–630. <https://doi.org/10.1109/CVPR.2010.5540156>
- [4] Taro Aoki, Takashi Murashima, Yoshihisa Asao, Toshihiro Nakae, and Masayoshi Yamaguchi. 1997. Development of high-speed data transmission equipment for the full-depth remotely operated vehicle “KAIKO”. In *Oceans ’97. MTS/IEEE Conference Proceedings*, Vol. 1. IEEE, 87–92.
- [5] Ching-Hang Chen and Deva Ramanan. 2017. 3D Human Pose Estimation = 2D Pose Estimation + Matching. In *2017 IEEE Conference on Computer Vision and Pattern Recognition (CVPR)*. 5759–5767. <https://doi.org/10.1109/CVPR.2017.610>
- [6] Kevin J DeMarco, Michael E West, and Ayanna M Howard. 2014. Underwater human-robot communication: A case study with human divers. In *2014 IEEE International Conference on Systems, Man, and Cybernetics (SMC)*. IEEE, 3738–3743.

- [7] Jia Deng, Wei Dong, Richard Socher, Li-Jia Li, Kai Li, and Li Fei-Fei. 2009. ImageNet: A large-scale hierarchical image database. In *2009 IEEE Conference on Computer Vision and Pattern Recognition*. 248–255. <https://doi.org/10.1109/CVPR.2009.5206848>
- [8] Jiankang Deng, Jia Guo, Evangelos Ververas, Irene Kotsia, and Stefanos Zafeiriou. 2020. Retinaface: Single-shot multi-level face localisation in the wild. In *2020 IEEE/CVF Conference on Computer Vision and Pattern Recognition (CVPR)*. 5203–5212. <https://doi.org/10.1109/CVPR42600.2020.00525>
- [9] Gregory Dudek, Philippe Giguere, Chris Prahacs, Shane Saunderson, Junaed Sattar, Luz-abril Torres-Mendez, Michael Jenkin, Andrew German, Andrew Hogue, Arlene Ripsman, Jim Zacher, Evangelos Milios, Hui Liu, Pifu Zhang, Marti Buehler, and Christina Georgiades. 2007. AQUA: An Amphibious Autonomous Robot. *Computer* 40, 1 (2007), 46–53. <https://doi.org/10.1109/MC.2007.6>
- [10] e-con Systems™. 2016. Tara – USB 3.0 Stereo Camera. <https://www.e-consystems.com/3D-USB-stereo-camera.asp>
- [11] Cameron Fabbri, Md Jahidul Islam, and Junaed Sattar. 2018. Enhancing Underwater Imagery Using Generative Adversarial Networks. In *2018 IEEE International Conference on Robotics and Automation (ICRA)*. 7159–7165. <https://doi.org/10.1109/ICRA.2018.8460552>
- [12] Martin A. Fischler and Robert C. Bolles. 1981. Random Sample Consensus: A Paradigm for Model Fitting with Applications to Image Analysis and Automated Cartography. *Commun. ACM* 24, 6 (jun 1981), 381–395. <https://doi.org/10.1145/358669.358692>
- [13] Michael Fulton, Chelsey Edge, and Junaed Sattar. 2022. Robot Communication Via Motion: A Study on Modalities for Robot-to-Human Communication in the Field. *ACM Transactions on Human Robot Interaction*. Accepted for publication. 11, 15 (June 2022), 1–40. Issue 2.
- [14] Michael Fulton, Jungseok Hong, and Junaed Sattar. 2022. Using Monocular Vision and Human Body Priors for AUVs to Autonomously Approach Divers. In *2022 International Conference on Robotics and Automation (ICRA)*. 1076–1082. <https://doi.org/10.1109/ICRA46639.2022.9811905>
- [15] Philippe Giguere, Yogesh Girdhar, and Gregory Dudek. 2013. Wide-Speed Autopilot System for a Swimming Hexapod Robot. In *2013 International Conference on Computer and Robot Vision*. 9–15. <https://doi.org/10.1109/CRV.2013.13>
- [16] Ross Girshick. 2015. Fast R-CNN. In *2015 IEEE International Conference on Computer Vision (ICCV)*. 1440–1448. <https://doi.org/10.1109/ICCV.2015.169>
- [17] Kaiming He, Xiangyu Zhang, Shaoqing Ren, and Jian Sun. 2015. Spatial Pyramid Pooling in Deep Convolutional Networks for Visual Recognition. *IEEE Transactions on Pattern Analysis and Machine Intelligence* 37, 9 (2015), 1904–1916. <https://doi.org/10.1109/TPAMI.2015.2389824>
- [18] Kaiming He, Xiangyu Zhang, Shaoqing Ren, and Jian Sun. 2016. Deep Residual Learning for Image Recognition. In *2016 IEEE Conference on Computer Vision and Pattern Recognition (CVPR)*. 770–778. <https://doi.org/10.1109/CVPR.2016.90>
- [19] Andrew G Howard. 2013. Some Improvements on Deep Convolutional Neural Network Based Image Classification. *arXiv preprint arXiv:1312.5402* (2013).
- [20] Jimin Hwang, Neil Bose, and Shuangshuang Fan. 2019. AUV Adaptive Sampling Methods: A Review. *Applied Sciences* 9, 15 (2019). <https://doi.org/10.3390/app9153145>
- [21] Md Jahidul Islam, Marc Ho, and Junaed Sattar. 2018. Dynamic Reconfiguration of Mission Parameters in Underwater Human-Robot Collaboration. In *2018 IEEE International Conference on Robotics and Automation (ICRA)*. IEEE, 6212–6219.
- [22] Md Jahidul Islam, Marc Ho, and Junaed Sattar. 2018. Understanding Human Motion and Gestures for Underwater Human-Robot Collaboration. *Journal of Field Robotics (JFR)* (2018), 1–23. <https://doi.org/10.1002/rob.21837>
- [23] Md Jahidul Islam, Peigen Luo, and Junaed Sattar. 2020. Simultaneous Enhancement and Super-Resolution of Underwater Imagery for Improved Visual Perception. In *Robotics: Science and Systems (RSS)*. Corvallis, Oregon, USA. <https://doi.org/10.15607/RSS.2020.XVI.018>
- [24] Tsung-Yi Lin, Piotr Dollár, Ross Girshick, Kaiming He, Bharath Hariharan, and Serge Belongie. 2017. Feature Pyramid Networks for Object Detection. In *2017 IEEE Conference on Computer Vision and Pattern Recognition (CVPR)*. 936–944. <https://doi.org/10.1109/CVPR.2017.106>
- [25] Xiabing Liu, Wei Liang, Yumeng Wang, Shuyang Li, and Mingtao Pei. 2016. 3D head pose estimation with convolutional neural network trained on synthetic images. In *2016 IEEE International Conference on Image Processing (ICIP)*. 1289–1293. <https://doi.org/10.1109/ICIP.2016.7532566>
- [26] Gregory P. Meyer, Shalini Gupta, Iuri Frosio, Dikpal Reddy, and Jan Kautz. 2015. Robust Model-Based 3D Head Pose Estimation. In *2015 IEEE International Conference on Computer Vision (ICCV)*. 3649–3657. <https://doi.org/10.1109/ICCV.2015.416>
- [27] Mahyar Najibi, Pouya Samangouei, Rama Chellappa, and Larry S. Davis. 2017. SSH: Single Stage Headless Face Detector. In *2017 IEEE International Conference on Computer Vision (ICCV)*. 4885–4894. <https://doi.org/10.1109/ICCV.2017.522>
- [28] Morgan Quigley, Ken Conley, Brian Gerkey, Josh Faust, Tully Foote, Jeremy Leibs, Rob Wheeler, and Andrew Y Ng. 2009. ROS: an open-source Robot Operating System. In *ICRA Workshop on Open Source Software*, Vol. 3. Kobe, Japan, 5.
- [29] Nataniel Ruiz, Eunji Chong, and James M. Rehg. 2018. Fine-Grained Head Pose Estimation Without Keypoints. In *2018 IEEE/CVF Conference on Computer Vision and Pattern Recognition Workshops (CVPRW)*. 2155–215509. <https://doi.org/10.1109/CVPRW.2018.00281>
- [30] Mark Sandler, Andrew Howard, Menglong Zhu, Andrey Zhmoginov, and Liang-Chieh Chen. 2018. MobileNetV2: Inverted Residuals and Linear Bottlenecks. In *2018 IEEE/CVF Conference on Computer Vision and Pattern Recognition*. 4510–4520. <https://doi.org/10.1109/CVPR.2018.00074>
- [31] Junaed Sattar, Eric Bourque, Philippe Giguere, and Gregory Dudek. 2007. Fourier tags: Smoothly degradable fiducial markers for use in human-robot interaction. In *Fourth Canadian Conference on Computer and Robot Vision (CRV '07)*. 165–174. <https://doi.org/10.1109/CRV.2007.34>
- [32] A. Vasilijevic, P. Calado, F. Lopez-Castejon, D. Hayes, N. Stilinovic, D. Nad, F. Mandic, P. Dias, J. Gomes, J. C. Molina, A. Guerrero, J. Gilabert, N. Miskovic, Z. Vukic, J. Sousa, and G. Georgiou. 2015. Heterogeneous robotic system for underwater oil spill survey. In *OCEANS 2015 - Genova*. 1–7. <https://doi.org/10.1109/OCEANS-Genova.2015.7271492>
- [33] Jianfeng Wang, Ye Yuan, and Gang Yu. 2017. Face Attention Network: An Effective Face Detector for the Occluded Faces. *arXiv preprint arXiv:1711.07246* (2017).
- [34] Youya Xia and Junaed Sattar. 2019. Visual Diver Recognition for Underwater Human-Robot Collaboration. In *2019 International Conference on Robotics and Automation (ICRA)*. 6839–6845. <https://doi.org/10.1109/ICRA.2019.8794290>
- [35] Shifeng Zhang, Xiangyu Zhu, Zhen Lei, Hailin Shi, Xiaobo Wang, and Stan Z. Li. 2017. S³FD: Single Shot Scale-Invariant Face Detector. In *2017 IEEE International Conference on Computer Vision (ICCV)*. 192–201. <https://doi.org/10.1109/ICCV.2017.30>